Proc. 15th Int. Conference on Defects Recognition, Imaging and Physics in Semiconductors, Warsaw, Poland 2013

Kelvin Force Microscopy Characterization of Corona Charged Dielectric Surfaces

D. Marinskiy[a], P. Edelman[a] and A.D. Snider[b]
[a]Semilab SDI, 10770N. 46th St., Ste E700, Tampa, FL, USA
[b]University of South Florida, 4202 East Fowler Avenue, Tampa FL, USA

Ionic diffusion of $(H_2O)_n^+$ and CO_3^- on SiO_2 surfaces has been quantified using Kelvin force microscopy measurement of ion distribution change after small spot corona charge. For both positive and negative ionic species, the concentration profiles versus time follow the two-dimensional surface diffusion enabling a determination of corresponding diffusion coefficients. On a thermally grown SiO_2 surface, diffusion coefficients of $(H_2O)_n^+$ and CO_3^- ions were 2.2×10^{-11} cm^2/s and 4.8×10^{-12} cm^2/s, respectively. On a chemically cleaned SiO_2 surface, diffusion coefficients of $(H_2O)_n^+$ and CO_3^- ions were 7.5×10^{-9} cm^2/s and 2.4×10^{-9} cm^2/s, respectively. Mathematical analysis of the surface potential decay yields an additional parameter — capacitance equivalent thickness.

DOI: 10.12693/APhysPolA.125.997
PACS: 77.55.–g, 73.61.–r, 68.37.Ps, 73.25.+i

1. Introduction

The corona-Kelvin based technique has been used as a non-contact, preparation free replacement of MOS and Schottky barrier capacitance–voltage (CV) measurements. It allows quantification of dielectric and interface properties such as dielectric capacitance and electrical thickness [1–4], density of interface states [2–4], and leakage across the dielectric [2–6]. Traditionally, a large spot corona-Kelvin approach is applied to unpatterned monitor wafers with blanket dielectric layers [2, 4, 5]. A miniaturization of both the Kelvin probe and corona deposition area has been introduced that extended the corona-Kelvin metrology to small spot measurements on product (i.e. patterned) silicon IC wafers and specifically to scribe-line test sites, which are 100 μm $\times$ 100 μm or smaller [4, 7]. Modified Kelvin force microscopy (KFM) with a probe of about 10 μm is used for surface potential measurements while the corona deposition diameter is reduced below 100 μm by employing a small aperture corona gun with electrostatic ion focusing [7].

In large spot corona-Kelvin measurements the surface potential is stable after corona charge deposition providing that the leakage current across dielectric is small enough not to neutralize the corona charge. As the corona deposition area is reduced below 100 μm, the surface potential on some dielectrics begins to exhibit a characteristic time decay (Fig. 1) that is related to a different phenomenon. Our work demonstrates that the origin of this potential decay is the lateral diffusion of corona ions away from the center of deposition. We analyze the rate of potential decay as a two-dimensional diffusion mechanism.

In this paper we present results of ionic diffusion on two types of SiO_2 surfaces, i.e. the surface after thermal oxidation and the surface after chemical cleaning. The experimental surface potential distribution profiles are analyzed using fundamental and modified solutions to the diffusion equation. A modified solution accounts for a non δ-function initial corona distribution. Lastly, an exact mathematical solution is presented. We demonstrate that the analysis of the surface potential decay yields two important parameters: capacitance equivalent thickness of the dielectric, CET, and diffusion coefficient of corona ions on the dielectric surface.

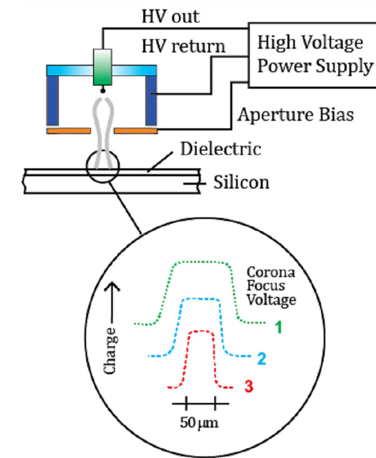

Fig. 1. Schematic drawing of apparatus used for deposition of corona charge on a dielectric surface. Increasing corona bias voltage $1 < 2 < 3$ decreases the diameter of corona spot.

2. Experimental

2.1. Sample preparation

P-type silicon wafers with a nominal 100 Å thermal SiO_2 layer were used in this study. Wafer resistivity was 8–12 Ωcm. One wafer was measured without additional surface treatment. The other was treated in SC1 solution (Standard Clean 1, $NH_4OH : H_2O_2 : H_2O = 1 : 1 : 5$ at 80 °C for 10 min) followed by a DI water rinse. SC1 cleaning is commonly used in silicon IC processing and is known to produce an –OH terminated SiO_2 surface [8, 9].

2.2. Measurement apparatus

2.2.1. Deposition of corona ions

Corona ions are generated by a corona discharge in air under atmospheric pressure. The corona apparatus consists of a point electrode in a charge confining cylinder. A high potential of 3 to 10 kV is applied to the point electrode. A wafer is placed on a grounded chuck and a 500 μm aperture is placed between the electrode and the wafer to control the area of corona charge deposition. Corona apparatus is schematically shown in Fig. 1. Positive ions, $(H_2O)_n^+$, are generated under positive bias conditions, and negative ions, CO_3^-, are generated under negative bias conditions [10, 11].

A corona charge diameter of ≈ 80 μm was achieved using electrostatic focusing, i.e. by application of ion repelling bias voltage to the aperture, see the inset in Fig. 1. Aperture bias voltage was ≈ 300 V. Surface ion density was controlled by controlling high voltage applied to the point electrode and the charging time. Initial ion density was in the range 0.4–0.6 μC/cm^2. For an SiO_2 dielectric this corresponds to an electric field of 1.2–1.6 MV/cm, i.e. much lower than the tunneling field range for charge leakage across SiO_2 dielectric [4, 5, 12] that could neutralize the corona charge.

It has been reported [13–16] that surface conductivity of SiO_2 is a strong function of humidity. One can expect that ionic diffusion on the surface also depends on humidity. Therefore for an accurate comparison of the two SiO_2 surface conditions experiments were performed in a clean room with controlled temperature and humidity at 40% RH.

2.2.2. Measurements of surface potential

Kelvin force microscopy (KFM) is used for surface potential measurements. A probe of 10 μm diameter enables measurements of surface potential distribution with high spatial resolution. The probe operates at a resonance frequency range above 100 kHz, enabling fast response time. Measurement accuracy below 0.5 mV is achieved at a probe to surface distance of 1 μm. KFM measurements were done on a FAaST 300 SL system [17].

The surface potential is measured before and after deposition of the corona charge. The change in surface potential is related to the surface density of ions as

$$qN(r,t) = C\Delta V_{\mathrm{CPD}}(r,t), \quad (1)$$

where q is the elementary charge, r is the distance from the center of the corona deposition area, $N(r,t)$ is the concentration of ions on dielectric surface [cm^{-2}], C is the capacitance per unit surface area [F cm^{-2}], and $\Delta V_{\mathrm{CPD}}(r,t)$ is the change in the surface potential with respect to the value before corona charging [V]. For an oxide/semiconductor interface, the total capacitance includes capacitance of the dielectric layer C_{diel} and the capacitance of semiconductor space charge layer C_{SC} [18]: $C^{-1} = C_{\mathrm{diel}}^{-1} + C_{\mathrm{SC}}^{-1}$. Under surface accumulation or inversion conditions $C_{\mathrm{SC}} \gg C_{\mathrm{diel}}$ and therefore the capacitance is approximately equal to the dielectric capacitance, C_{diel}. Capacitance of the space charge layer is also increased for highly doped wafers and by illuminating the sample with high intensity light [2]. For example, capacitance of a 100 Å SiO_2 dielectric is ≈ 0.35 μF/cm^2 and the conditions $C_{\mathrm{SC}} \gg C_{\mathrm{diel}}$ is satisfied when silicon surface potential is < -0.2 V (deep accumulation) or > 0.8 V (strong inversion). Therefore measuring under strong illumination conditions is important to minimize contribution of C_{SC} to the total capacitance. In the analysis that follows, we approximate $C \approx C_{\mathrm{diel}}$.

3. Theory and calculation

The ion density $N(r,\theta,z,t)$ spreads according to the diffusion equation $\frac{\partial N}{\partial t} = \nabla \cdot (\overleftrightarrow{\boldsymbol{D}} \cdot \nabla N)$. The vertical component of diffusion is negligible and the phenomenon is modeled as radially symmetric. The governing equation becomes

$$\frac{\partial N}{\partial t} = D\nabla^2 N(r,t) = D\left(\frac{\partial^2 N}{\partial r^2} + \frac{1}{r}\frac{\partial N}{\partial r}\right). \quad (2)$$

The solution depends on initial conditions, i.e. initial ion distribution and dose. We will discuss three cases below.

3.1. Fundamental solution

For an initial δ-function distribution the solution has a Gaussian form

$$N(r,t) = \frac{N_0}{4\pi Dt}\exp\left(\frac{-r^2}{4Dt}\right), \quad (3)$$

where N_0 is the initial dose of corona ions, r is the radius from the center of ion deposition, t is the time after ion deposition, and D is the surface diffusion coefficient.

The change of the surface potential distribution is described by

$$\Delta V_{\mathrm{CPD}}(r,t) = \frac{qN_0}{C_{\mathrm{diel}} 4\pi Dt}\exp\left(\frac{-r^2}{4Dt}\right). \quad (4)$$

Fitting the experimental surface potential distribution to Eq. (4) enables extraction of the diffusion coefficient, D. Moreover, knowledge of the dielectric capacitance, C_{diel}, and initial ion dose, N_0, is not required for diffusion coefficient calculation if only the exponential term in Eq. (4) is considered.

3.2. Modified Gaussian distribution

A modified solution is proposed to account for a non δ-function initial distribution. If the initial distribution can be approximated by a Gaussian distribution, then a modified solution is

$$\Delta V_{\mathrm{CPD}}(r,t) = \frac{qN_0}{C_{\mathrm{diel}} 4\pi D(t+\tau)}\exp\left(\frac{-r^2}{4D(t+\tau)}\right). \quad (5)$$

Justification for the modified solution is as follows: at time $t = \tau$ the δ-function will look like the initial surface potential distribution. So the solution $\Delta V_{\mathrm{CPD}}(r,t)$ can be approximated as a fundamental solution (Eq. (4)) starting τ seconds earlier. This is shown schematically in Fig. 2. Parameter τ can be determined from the time dependence of the pre-exponential term in Eq. (5).

3.3. Exact solution to 2D diffusion equation

Deposition of corona ions results in a uniform distribution over a circle of radius $R = 40$ μm. The wafer diameter is 300 mm, i.e. much larger than the diameter

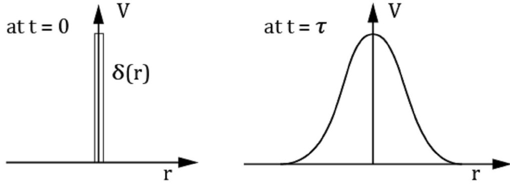

Fig. 2. Corona ion distribution at time $t = 0$ and at time $t = \tau$. After τ seconds the initial δ-distribution changes to Gaussian.

of the corona ion deposition area. It can be taken as infinitely remote for the duration of diffusion. The initial ion density produces the initial surface charge density $Q_0 = q \times N_0$. R and N_0 are determined by the charging conditions.

The solution to the diffusion Eq. (2) satisfying the initial condition is given by USFKAD [19]:

$$N(r,t) = N_0 \int_0^{\infty} A(k) J_0(kr) \mathrm{e}^{-k^2 Dt} \mathrm{d}k,$$

where

$$A(k) = \int_0^R J_0(kr) kr \, \mathrm{d}r = R J_1(kR). \tag{6}$$

The voltage dependence at $r = 0$ can be described as (Appendix A):

$$\Delta V(t) = \frac{h}{\varepsilon\varepsilon_0} q N_0 - \frac{h}{\varepsilon\varepsilon_0} q (N_0 - N_\infty) \mathrm{e}^{-R^2/4Dt}, \tag{7}$$

where $N_\infty = N(0,\infty)$ is the ion density at time $t = \infty$, h is the thickness of the dielectric layer, R is the radius of initial corona charge deposition circle.

From Eq. (7) it follows that the plot of $t \times \ln(-t^2 \dot{V}(t))$ versus t, defined as a Snider plot, should be a straight line (Appendix A):

$$t \ln\left(-t^2 \dot{V}(t)\right) = \left(\ln \frac{q(N_0 - N_\infty) R^2 h}{4\varepsilon\varepsilon_0 D}\right) t - \frac{R^2}{4D}$$

$$= \text{slope} \cdot t + \text{intercept}. \tag{8}$$

The slope and intercept can be estimated by linear regression, enabling the extraction of D and h:

$$D = \frac{-R^2}{4 \times \text{intercept}}, \tag{9}$$

$$h = \left(\Delta V(t) + \frac{4D}{R^2} \mathrm{e}^{\text{slope}} \mathrm{e}^{\text{intercept}/t}\right) \frac{\varepsilon\varepsilon_0}{q N_0}. \tag{10}$$

4. Results and discussion

Time evolution of the surface potential distribution after charging with positive $(H_2O)_n^+$ and negative CO_3^- ions are shown in Figs. 3, 4.

4.1. Diffusion coefficient from the fundamental and modified solutions

Individual voltage–distance profiles are fitted to the fundamental (Eq. (4)) and the modified (Eq. (5)) solutions. Parameter τ for the modified solution is obtained from the voltage transient at $r = 0$, i.e. $V(0,t)$. Figure 5 shows fitting of $\Delta V(0,t)$ to $1/(t+\tau)$ for SC1 cleaned and thermal SiO_2 surfaces. Table I summarizes τ values

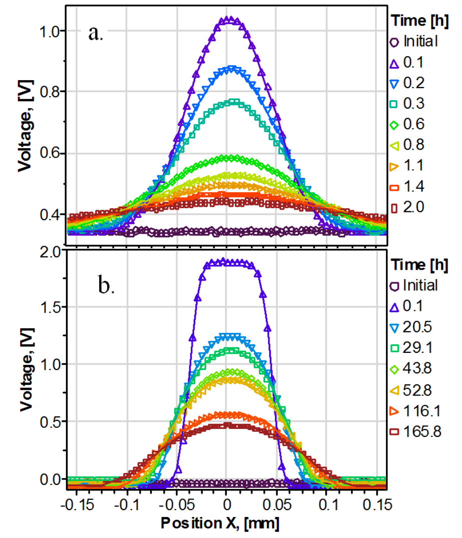

Fig. 3. Kelvin force microscopy profiles of the surface potential distribution for different times after deposition of positive corona ions, $(H_2O)_n^+$, on SC1 cleaned (a) and thermal (b) SiO_2 surfaces.

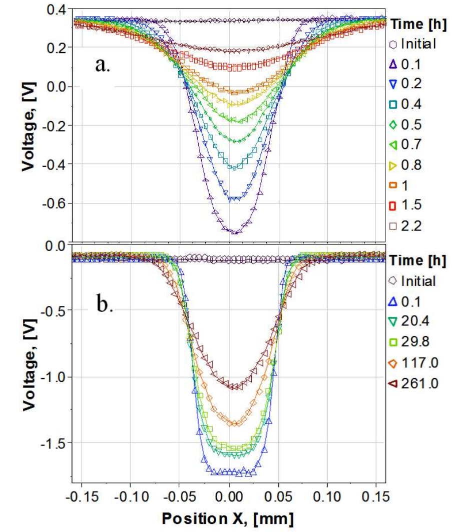

Fig. 4. KFM profile of the surface potential distribution versus position X for different times after deposition of negative corona ions, CO_3^-, on SC1 cleaned (a) and thermal (b) SiO_2 surfaces.

obtained for each surface and corona ion condition. Diffusion coefficients calculated for each voltage distribution profile are shown in Figs. 6 and 7.

Diffusion coefficients calculated from the fundamental solution show a characteristic time dependence. This is due to the simplified assumption of the initial δ-function corona ion distribution. It can be seen (Figs. 6, 7) that for longer times the calculated diffusion coefficient saturates and approaches values obtained from the modified solution. This is expected since for longer times $t \gg \tau$ and therefore Eqs. (4) and (5) should give a similar dif-

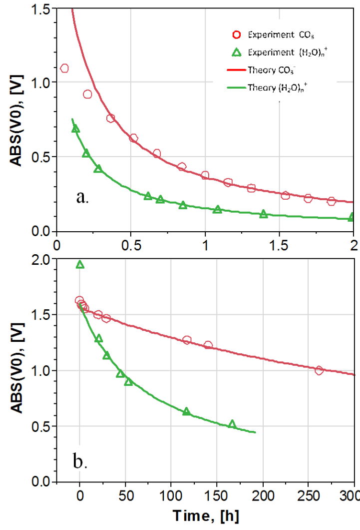

Fig. 5. Voltage transient at $r = 0$ for SC1 cleaned (a) and thermal (b) SiO_2 surfaces. Fitting to $1/(t+\tau)$ enables extraction of the parameter τ.

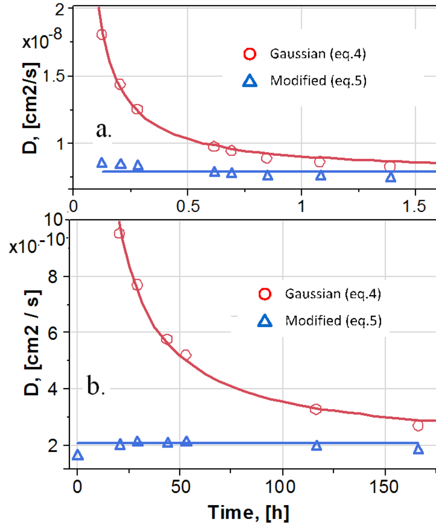

Fig. 6. Diffusion coefficient for each voltage distribution profile shown in Fig. 3 for positive corona ions, $(H_2O)_n^+$, on SC1 cleaned (a) and thermal (b) SiO_2 surfaces.

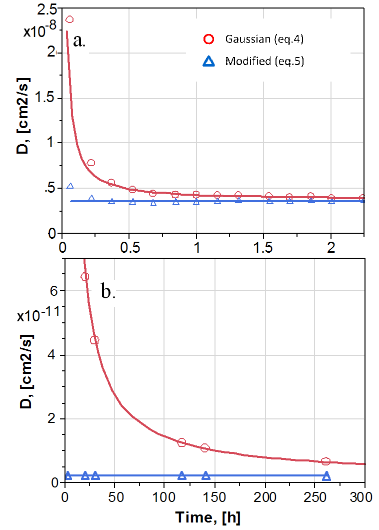

Fig. 7. Diffusion coefficient for each voltage distribution profile shown in Fig. 4 for negative corona ions, CO_3^-, on SC1 cleaned (a) and thermal (b) SiO_2 surfaces.

fusion coefficient. We note that for the SC1 cleaned SiO_2 surface parameter τ is less than 0.2 h (Table I) while the change of surface potential distribution is monitored for 2 h (Figs. 3a, 4a). The condition $t \gg \tau$ is satisfied and indeed diffusion coefficients obtained from the fundamental and modified solutions show approximately the same values.

On the thermal SiO_2 surface, parameter τ is 74 h and 482 h for diffusion of positive and negative corona ions respectively, while the change of surface potential distribution is monitored for up to 300 h. The longest measurement time is less than $2\times\tau$ and diffusion coefficient obtained from the fundamental and modified solutions

TABLE I

Parameter τ obtained from the fitting of $V(0,t)$ to $1/(t+\tau)$.

Ion	Surface	τ [h]
$(H_2O)_n^+$	SC1	0.14
	thermal	74.12
CO_3^-	SC1	0.19
	thermal	482.1

still shows a difference. For positive corona ions the difference is ≈ 1.5 times while for the negative corona ions the difference is ≈ 3 times. Nevertheless, from the fundamental solution the diffusion coefficient can be obtained by extrapolation to time $t = \infty$.

Diffusion coefficients obtained from the fundamental and modified solutions are summarized in Table II. Ionic diffusion on the SC1 treated SiO_2 surface is much faster than that on SiO_2 after thermal processing. We observed more than 2 orders of magnitude increase in the diffusion coefficient on the SC1 treated surface.

TABLE II

Diffusion coefficient [cm^2/s] obtained from the fundamental and modified solutions.

Ion	Surface	Fundamental (Eq. (4))	Modified (Eq. (5))
$(H_2O)_n^+$	SC1	$(8.2\pm0.1)\times10^{-9}$	$(7.8\pm0.2)\times10^{-9}$
	thermal	$(2.8\pm0.2)\times10^{-11}$	$(2.1\pm0.1)\times10^{-11}$
CO_3^-	SC1	$(4.2\pm0.1)\times10^{-9}$	$(3.6\pm0.8)\times10^{-9}$
	thermal	$(9.8\pm0.1)\times10^{-12}$	$(2.5\pm0.1)\times10^{-12}$

The diffusion coefficient for $(H_2O)_n^+$ is higher than that for CO_3^-. The higher diffusion coefficient for $(H_2O)_n^+$ is consistent with its smaller atomic weight.

Lastly, the simplifying assumption of the initial δ-function distribution is justified by the ease of the experimental data analysis and from the fact that for longer times ions spread over a distance much larger than the initial corona distribution, and therefore the initial corona distribution can be well approximated by the δ-function.

4.2. Diffusion coefficient and CET from the exact solution

Solution of diffusion Eq. (2) using USFKAD predicts that the plot of $t \times \ln(-t^2\dot{V}(t))$ versus t, defined as a Snider plot, should be a straight line. Data for SC1 cleaned and thermal SiO_2 surfaces are shown in Fig. 8. Let us note the excellent linearity of the data. R^2 of the linear fit is > 0.997 for all cases (Table III). The diffusion coefficient and CET are calculated using the intercept and slope of the linear fit (Eqs. (9), (10)) and the results are summarized in Table III.

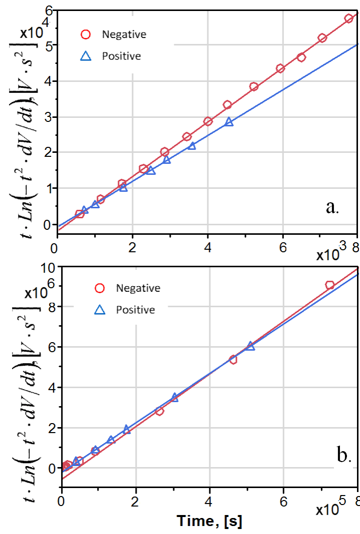

Fig. 8. Snider plot for (a) SC1 cleaned and (b) thermal SiO_2 surfaces.

TABLE III

Diffusion coefficient and CET obtained from the exact mathematical solution.

Ion	Surface	D [cm^2/s] (Eq. (9))	R^2	CET [Å]
$(H_2O)_n^+$	SC1	$(7.5 \pm 0.5) \times 10^{-9}$	0.9995	94.7
	thermal	$(2.2 \pm 0.3) \times 10^{-11}$	0.9999	97.7
CO_3^-	SC1	$(2.4 \pm 0.2) \times 10^{-9}$	0.9994	92.1
	thermal	$(4.8 \pm 0.9) \times 10^{-12}$	0.9979	95.4

Initial conditions include the radius of the corona deposition area, R, and the initial ion density, N_0. From Eqs. (9) and (10) it follows that the calculation of diffusion coefficient only depends on the radius R, while the calculation of CET only depends on N_0. This simplifies the experimental setup: if one is interested in a diffusion coefficient, then only the radius of the initial corona deposition area must be known; if one is interested in a CET parameter, then only the initial corona dose must be known/calibrated.

CET calculated for the thermal and SC1 cleaned SiO_2 surface shows good agreement with the nominal dielectric thickness of 100 Å. The small difference observed for positive and negative bias conditions is attributed to the contribution of the silicon space charge layer, while the difference between the SC1 cleaned and thermal SiO_2 surfaces is attributed to slight etching of SiO_2 by SC1 solution [20, 21].

The diffusion coefficient obtained from the solution of the 2D diffusion equation shows good agreement with the data obtained from the analysis of voltage distribution profiles using the fundamental and modified solutions.

5. Conclusions

We have presented a method to quantify ion surface diffusion coefficients on dielectric surfaces. The ions are deposited onto the dielectric surface by small spot corona charging and the charge profile is measured as a function of time by the Kelvin force microscopy measurement of the surface voltage.

We found that for both positive, $(H_2O)_n^+$, and negative, CO_3^-, ionic species the concentration profile versus time follows two-dimensional surface diffusion enabling calculation of the corresponding surface diffusion coefficients. We have analyzed experimental data using three approaches, which were different by assumption of initial ion distribution, namely, fundamental, modified, and exact solutions. Diffusion coefficients calculated using each approach show good agreement with each other. These coefficients are different for as grown oxide and chemically cleaned SiO_2 surfaces. On a thermally grown SiO_2 surface, the diffusion coefficients of $(H_2O)_n^+$ and CO_3^- ions were 2.2×10^{-11} cm^2/s and 4.8×10^{-12} cm^2/s, respectively. On a chemically cleaned SiO_2 surface, the diffusion coefficients of $(H_2O)_n^+$ and CO_3^- ions were 7.5×10^{-9} cm^2/s and 2.4×10^{-9} cm^2/s, respectively.

The exact solution yields an addition parameter — dielectric thickness, CET. The CET calculation depends only on the initial corona dose, while diffusion coefficient calculation depends only on the radius of corona deposition area.

The present findings are of importance for fundamental understanding of the corona-Kelvin measurements on small test sites below 100 μm that are used in silicon IC manufacturing. The method can be expanded to dielectric surfaces other than SiO_2.

Acknowledgments

The authors wish to thank M. Wilson and J. Lagowski for the critical review of the manuscript.

Appendix A. Solution to 2D diffusion with specific boundary conditions

A.1. Initial conditions

Corona ions are deposited over a circle of radius $R = 40$ μm. Ion density is uniform and is equal to N_0. Corresponding surface charge density is $Q_0 = q \times N_0$. The wafer diameter is 300 mm, i.e. much larger than the diameter of the corona ion deposition area.

2D diffusion equation is

$$\frac{\partial N}{\partial t} = D\nabla^2 N(r,t) = D\left(\frac{\partial^2 N}{\partial r^2} + \frac{1}{r}\frac{\partial N}{\partial r}\right). \tag{A1}$$

Relation between ion density and surface potential is

$$qN(r,t) = C_{\mathrm{diel}}\Delta V_{\mathrm{CPD}}(r,t). \tag{A2}$$

A.2. Solution

Solution to the diffusion Eq. (A1) satisfying the initial conditions is given by USFKAD [19]:

$$N(r,t) = N_0\int_0^\infty A(k)J_0(kr)\mathrm{e}^{-k^2Dt}\,\mathrm{d}k,$$

where

$$A(k) = \int_0^R J_0(kr)kr\,\mathrm{d}r = RJ_1(kR), \tag{A3}$$

where J and J_1 are the Bessel functions of the first kind of orders zero and one, respectively.

At $r = 0$, i.e. in the center of corona ion deposition, the charge density simplifies to

$$N(0,t) = N_0\int_0^\infty RJ_1(kR)\mathrm{e}^{-k^2Dt}\,\mathrm{d}k = N_0\int_0^\infty J_1(z)\mathrm{e}^{-z^2Dt/R^2}\,\mathrm{d}z. \tag{A4}$$

Integration by parts produces an equivalent expression

$$N(0,t) = N_0 - \frac{4D^2t^2N_0}{R^4}\int_0^\infty z^2J_1(z)\mathrm{e}^{-z^2Dt/R^2}\,\mathrm{d}z. \tag{A5}$$

Examination reveals that the integral in Eq. (A5) can be reproduced in Eq. (A4) by differentiating with respect to time, so that in fact $N(r,t)$ satisfies the solvable ordinary differential equation

$$\frac{\mathrm{d}N(0,t)}{\mathrm{d}t} = \frac{R^2}{4Dt^2}N(0,t) - \frac{N_0R^2}{4Dt^2} \Rightarrow N(0,t) = N_0 - [N_0 - N_\infty]\mathrm{e}^{-R^2/4Dt}. \tag{A6}$$

The value $N_\infty = N(0,\infty)$ would be zero if the finite charge was diffused over an idealized infinite region, but we retain it here to enable curve-fitting.

Combining Eqs. (A2) and (A6) gives

$$\Delta V(t) = \frac{h}{\varepsilon\varepsilon_0}qN_0 - \frac{h}{\varepsilon\varepsilon_0}q(N_0 - N_\infty)\mathrm{e}^{-R^2/4Dt}. \tag{A7}$$

The derivative of Eq. (A7) is $\dot{V}(t) = \frac{\mathrm{d}V}{\mathrm{d}t} = -\frac{hq(N_0-N_\infty)R^2}{4\varepsilon Dt^2}\mathrm{e}^{-R^2/4Dt}$ and a little algebra produces the remarkable equation

$$t\ln\left(-t^2\dot{V}(t)\right) = \left(\ln\frac{q(N_0 - N_\infty)R^2h}{4\varepsilon\varepsilon_0 D}\right)t - \frac{R^2}{4D} = \mathrm{slope}\cdot t + \mathrm{intercept}. \tag{A8}$$

Thus the plot of $t \times \ln\left(-t^2\dot{V}(t)\right)$, defined as a Snider plot, should be a straight line, whose slope and intercept can be estimated by linear regression, enabling the extraction of D and h:

$$D = \frac{-R^2}{4\times\mathrm{intercept}}, \quad N_0 - N_\infty = \frac{1}{q}\frac{\varepsilon\varepsilon_0}{h}\frac{4D}{R^2}\mathrm{e}^{\mathrm{slope}}. \tag{A9}$$

As a result Eqs. (A7) and (A9) imply

$$h = \left(V(t) + \frac{h}{\varepsilon\varepsilon_0}q(N_0 - N_\infty)\mathrm{e}^{-R^2/4Dt}\right)\frac{\varepsilon\varepsilon_0}{qN_0} = \left(V(t) + \frac{4D}{R^2}\mathrm{e}^{\mathrm{slope}}\mathrm{e}^{\frac{\mathrm{intercept}}{t}}\right)\frac{\varepsilon\varepsilon_0}{qN_0}, \tag{A10}$$

enabling the calculation of h from the data. When $\varepsilon = \varepsilon(SiO_2)$ the calculated thickness corresponds to capacitance equivalent thickness, CET.

References

[1] D.K. Schroder, *Meas. Sci. Technol.* **12**, R16 (2001).

[2] D.K. Schroder, *Mater. Sci. Eng. B* **91-92**, 196 (2002).

[3] P. Edelman, A. Savtchouk, M. Wilson, J. D'Amico, J.N. Kochey, D. Marinskiy, J. Lagowski, *Europ. Phys. J. Appl. Phys.* **27**, 495 (2004).

[4] M. Wilson, D. Marinskiy, A. Byelyayev, J. D'Amico, A. Findlay, L. Jastrzebski, J. Lagowski, *ECS Trans.* **3**, 3 (2006).

[5] R. Williams, M.H. Woods, *J. Appl. Phys.* **44**, 1026 (1973).

[6] R.B. Comizzoli, *J. Electrochem. Soc.* **134**, 424 (1987).

[7] P. Edelman, D. Marinskiy, C. Almeida, J.N. Kochey, A. Byelyayev, M. Wilson, A. Savtchouk, J. D'Amico, A. Findlay, L. Jastrzebski, J. Lagowski, *Mater. Sci. Semicond. Proc.* **9**, 252 (2006).

[8] M.L. Green, M.-Y. Ho, B. Busch, G.D. Wilk, T. Sorsch, T. Conard, B. Brijs, W. Vandervorst, P.I. Räisänen, D. Muller, M. Bude, J. Grazul, *J. Appl. Phys.* **92**, 7168 (2002).

[9] W. Tsai, R.J. Carter, H. Nohira, M. Caymax, T. Conard, V. Cosnier, S. DeGendt, M. Heyns, J. Petry, O. Richard, W. Vandervorst, E. Young, C. Zhao, J. Maes, M. Tuominen, W.H. Schulte, E. Garfunkel, T. Gustafsson, *Microelectron. Eng.* **65**, 259 (2003).

[10] M.M. Shahin, *J. Chem. Phys.* **45**, 2600 (1966).

[11] M.M. Shahin, *Appl. Opt.* **8**, 106 (1969).

[12] D.K. Schroder, *Semiconductor Material and Device Characterization*, 2nd ed., Wiley, New York 1998, p. 481.

[13] J.A. Voorthuyzen, K. Keskin, P. Bergveld, *Surf. Sci.* **187**, 201 (1987).

[14] A.D. Martin, K.J. McLean, *J. Appl. Phys.* **48**, 2950 (1977).

[15] Y. Awakuni, J.H. Calderwood, *J. Phys. D, Appl. Phys.* **5**, 1038 (1972).

[16] J. D'Amico, Ph.D. thesis, University of South Florida, Tampa 2000.

[17] `http://www.semilab.hu/products/si/faast-300-sl` .

[18] S.M. Sze, *Physics of Semiconductor Devices*, Wiley, New York 1981, Ch. 9.

[19] S. Kadamani, A.D. Snider, "USFKAD: An Expert System for Partial Differential Equations", *Comp. Phys. Commun.* **176**, 62 (2007).

[20] S.D. Hossain, M.F. Pas, *J. Electrochem. Soc.* **140**, 3604 (1993).

[21] K.T. Lee, S. Raghavan, *Electrochem. Solid-State Lett.* **2**, 172 (1999).